Novel Boron-Containing, Nonclassical Antifolates: Synthesis and Preliminary Biological and Structural Evaluation†

Robert C. Reynolds,*,‡ Shiela R. Campbell,‡ Ralph G. Fairchild,§ Roy L. Kisliuk,|| Peggy L. Micca,§ Sherry F. Queener,⊥ James M. Riordan,‡ W. David Sedwick,# William R. Waud,‡ Adelaine K.W. Leung,‡,⊗ Richard W. Dixon,○ William J. Suling,‡ and David W. Borhani*,‡,⊗,○

Drug Discovery Division, Southern Research Institute, Birmingham, Alabama 35205, Medical Department, Brookhaven National Laboratory, Upton, New York 11973, Department of Biochemistry, Tufts University Sackler School of Graduate Biomedical Sciences, Boston, Massachusetts 02111, Department of Pharmacology and Toxicology, Indiana University School of Medicine, Indianapolis, Indiana 46202, Department of Medicine, Case Western Reserve University, Cleveland, Ohio 44106, Department of Chemistry, Abbott Bioresearch Center, Worcester, Massachusetts 01605

Received February 20, 2007

Two boron-containing, *ortho*-icosahedral carborane lipophilic antifolates were synthesized, and the crystal structures of their ternary complexes with human dihydrofolate reductase (DHFR) and dihydronicotinamide adenine dinucleotide phosphate were determined. The compounds were screened for activity against DHFR from six sources (human, rat liver, *Pneumocystis carinii*, *Toxoplasma gondii*, *Mycobacterium avium*, and *Lactobacillus casei*) and showed good to modest activity against these enzymes. The compounds were also tested for antibacterial activity against *L. casei*, *M. tuberculosis* $H_{37}Ra$, and three *M. avium* strains and for cytotoxic activity against seven different human tumor cell lines. Antibacterial and cytotoxic activity was modest, with one sample, the *closo*-carborane **4**, showing about 10-fold greater activity. The less toxic *nido*-carborane **2** was also tested as a candidate for boron neutron capture therapy, but showed poor tumor retention and low selectivity ratios for boron distribution in tumor tissue versus normal tissue.

Introduction

Although dihydrofolate reductase (DHFR[a]) has been a chemotherapeutic target in antibacterial, anticancer, and antiparasitic drug treatment for about 50 years, interest in new agents that target this crucial enzyme remains high.[1,2] In particular, ongoing research is focusing on understanding the specific interactions of antifolates with DHFR and structural modifications that improve selectivity of antifolates for anticancer,[3,4] antibacterial,[5] and antiparasitic targets.[6] More recently, antifolates have been used to ameliorate symptoms in autoimmune disorders,[7] and an approach to new insecticides has been reported that proposes targeting the DHFR from the tobacco budworm.[8]

Herein, we describe the preparation of two nonclassical, lipophilic 2,4-diamino-6-methylpyrimidine antifolates containing either a 5-(7,8-*nido*-dicarbaundecarboran-7-yl)methyl (**2**) or a 5-(1,2-*closo*-dicarbadodecarboran-1-yl)methyl (**4**) substituent (Scheme 1). This work is a continuation of our program focused on the study of steric tolerance in the binding site of DHFR.[9] These compounds were interesting for several reasons. First, the substitution of a carborane cage (e.g., *closo*-carborane **4**) in lipophilic antifolates has never been reported and would sterically approximate a phenyl substitution, where the aromatic ring is rotated in three-dimensional space.[10] Additionally, the *nido*-carborane **2** opens one face of the icosahedron, and the

Scheme 1. Preparation of Carboranes **2** and **4**; Structures of the *closo*-1,2-Carborane Cage and TMP

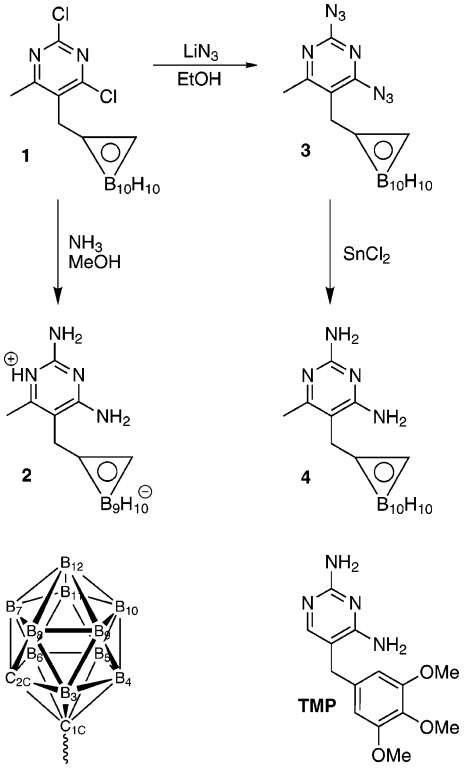

† Atomic coordinates and observed structure factors have been deposited at the Protein Data Bank with accession numbers 2C2T (compound **2**) and 2C2S (compound **4**).

* To whom correspondence should be addressed. For the chemistry and biological data: Robert C. Reynolds, Dept. of Organic Chemistry, Southern Research Institute, 2000 Ninth Ave. S., Birmingham, AL 35205. Tel.: 205-581-2454. Fax: 205-581-2877. E-mail: E-mail: reynolds@sri.org. For the crystallography and modeling: David W. Borhani, D. E. Shaw Research, LLC, 39th Floor, Tower 45, 120 West 45th Street, New York, New York 10036. Tel.: 212-478-0000. Fax: 212-478-0100. E-mail: david.borhani@alum.mit.edu.

‡ Southern Research Institute.

§ Brookhaven National Laboratory.

|| Tufts University.

⊥ Indiana University School of Medicine.

Case Western Reserve University.

⊗ Current Addresses: Dept. of Neurobiology, Harvard Medical School, Boston, MA 02115 (A.K.W.L.); D. E. Shaw Research, LLC, 39th Floor, Tower 45, 120 West 45th Street, New York, New York 10036 (D.W.B.).

○ Abbott Bioresearch Center.

[a] Abbreviations: ASA, solvent accessible surface area; BNCT, boron neutron capture therapy; DHFR, dihydrofolate reductase; FBS, fetal bovine serum; hDHFR, human DHFR; NADPH, dihydronicotinamide adenine dinucleotide phosphate; MIC, minimum inhibitory concentration; TMP, trimethoprim.

10.1021/jm0701977 CCC: $37.00
Published on Web 06/15/2007

Table 1. Carborane ^{13}C NMR Chemical Shifts

	carbon atom and chemical shift (ppm)							
cmpd	C-6	C-5	C-4	C-2	C(1) carborane	C(2) carborane	5-CH_2	6-CH_3
2	149.56	106.81	164.60	153.42	57.67	46.06	31.50	16.85
2 + DCl	149.65	107.05	164.76	153.70	57.68	47.05	31.81	16.99
4	164.55	100.14	163.14	161.34	77.19	64.05	32.40	21.71
4 + DCl	152.65	102.32	164.20	153.65	75.21	64.43	30.22	17.07

open face retains a negative charge. It was interesting to screen this derivative for DHFR inhibition because the altered carborane cage is no longer rotationally symmetrical and the negative charge of the *nido*-carborane would be placed proximal to the hydride donor, NADPH. It was also interesting to determine what effect these substitutions would have on enzyme binding and specificity for eukaryotic versus prokaryotic DHFR preparations as this substitution point in the 2,4-diamino-5-benzylpyrimidines is crucial for driving antibacterial selectivity.[11]

To gain further insight into how these nonclassical antifolates were accommodated by DHFR, we determined the crystal structures of both **2** and **4** bound to human DHFR (hDHFR), as the ternary complexes with NADPH.

These boron-containing antifolates were also potential candidates for boron neutron capture therapy (BNCT)[12−14] because they are low molecular weight, lipophilic compounds that contain a high percentage of boron. BNCT continues to be pursued as a possible cancer therapy, especially for inoperable brain tumors.[15] Data are also presented on boron tissue distribution of the less toxic *nido*-carborane **2** as a function of time after administration, and these data relate to the value of these agents as potential boron carriers for BNCT.

Chemistry

The preparation of the boron-containing antifolates **2** and **4** is shown in Scheme 1. The dichloropyrimidine **1**, which possesses the *closo*-1,2-carborane icosahedral cage, was synthesized according to known procedures.[16] Deboronation reaction[17] of *closo*-carborane **1** with ammonia/methanol in a bomb at 160−165 °C for 22 h to give a good yield (87%) of the *nido*-carborane **2** after isolation and purification by column chromatography. Compound **1** was also reacted with lithium azide in ethanol at reflux to give a 65% yield of the 2,4-diazidopyrimidine derivative **3**. The diazido derivative was promptly reduced using tin(II) dichloride[18] in methylene chloride. Workup and purification afforded the 2,4-diamino derivative (**4**) in 73% yield. The structure of **2** was determined by comparing the ^{13}C NMR spectra of compounds **2** and **4**, Table 1. The large upfield shift of 18−20 ppm in the carborane carbons in **2**, relative to carborane carbons of **4**, indicates the presence of a negative charge in the carborane ring. The site of protonation of the pyrimidine ring in **2** is the same as in **4** when **4** is treated with DCl; there is no change in **2** when treated with DCl; Table 1. The shifts of C6, C4, and 6-CH_3 show the hydrogen resides on N1. Furthermore, the broad B−H stretching bands for the *closo*-carboranes **3** and **4** appear at higher frequencies in the IR spectra by about 50 cm^{-1} than the carborane analog **2**, clearly indicating that **2** is indeed a *nido*-carborane.[19]

Results and Discussion

Biological Activity. The results of enzyme inhibition studies with carboranes **2** and **4** and several sources of DHFR are presented in Table 2. Carborane **4** tended to be the more potent inhibitor, being 100-, 12-, 58-, and 32- to 78-fold more potent than **2** against human, rat liver, *L. casei*, and *M. avium* DHFR, respectively. Both **2** and **4** had comparable activity against *T. gondii* DHFR, with IC_{50}s of 72 and 140 nM. Interestingly, the activity of **2** against the parasite enzyme compares quite favorably (65- to 208-fold more active) with its weaker activity against rat or hDHFR assayed under identical conditions.

Table 2. Inhibition of DHFR from Several Sources

	DHFR source and IC_{50} (μM)					
cmpd	human	rat liver	*P. carinii*	*T. gondii*	*M. avium*	*L. casei*
2	15	4.68	21.5	0.072	107 270[c]	1500
4	0.15	0.37	14	0.14	6.2 7.2[c]	26
TMP		133 26[b]	12	2.73	0.19	0.62
6-CH_3-TMP		>40[b]				
methotrexate[a]	0.02					0.006

[a] Control compound. [b] Ref 26. [c] Values represent results determined independently by another laboratory.

Four trends are apparent when **2** and **4** are compared to the standard antibacterial lipophilic antifolate trimethoprim (TMP; see Scheme 1), of which these carboranes are analogues (Table 2). First, both carboranes are noticeably more potent than TMP against *T. gondii* DHFR (20- to 40-fold). Second, both carboranes are more potent than TMP against the mammalian DHFRs, with carborane **4** exhibiting 100-fold improved activity against the rat enzyme. Third, the carboranes had (weak) activity equivalent to TMP when assayed against *P. carinii* DHFR. Fourth, both carboranes were much poorer inhibitors of the two bacterial DHFRs tested. All these activity differences likely result from differential accommodation of the active site of each DHFR to both the 6-CH_3 group and the carborane cages; each DHFR possesses a unique active site width and character (polar or nonpolar) of the amino acids proximal to the carborane cage.

The inhibition of the growth of *L. casei* and the mycobacterial strains by **2** and **4** correlated with results for DHFR inhibition in that **4** was the more potent inhibitor (Table 3). Only modest activity (minimum inhibitory concentration (MIC) of $>12.8 \leq 128$ μg/mL) was seen with **4** against *L. casei* and three of the four mycobacterial strains. The fourth strain, MAC NJ211, was inhibited by **4** in the range $>1.28 \leq 12.8$ μg/mL.

L. casei cannot produce dihydrofolate de novo and therefore requires folates for growth. Also, if the mechanism of action of **2** and **4** was primarily inhibition of DHFR, then thymidine would be expected to reverse the inhibition as long as other products of folate metabolism are present. The addition of 5-formyltetrahydrofolate to the growth medium will also bypass the metabolic blockage caused by DHFR inhibition. Therefore, we determined the effect of 100 μM thymidine and 0.1 mg/mL 6-(*R,S*)-5-formyltetrahydrofolate, alone and in combination, on the inhibition of growth by **2** and **4**. None of the attempts to reverse inhibition were successful. These results suggested that, at least for *L. casei*, **2** and **4** were not inhibiting growth primarily through the inhibition of DHFR and that other mechanisms of action likely were operative.

Both carboranes **2** and **4** were modestly active against a panel of tumor cell lines, with compound **4** showing on the order of

Table 3. Minimum Inhibitory Concentration (MIC) of **2** and **4**.

	MIC (μg/mL)				
			M. avium		
cmpd	*L. caseii*	*M. tuberculosis* MTB $H_{37}Ra$	MAC NJ128	MAC NJ211	MAC NJ3404
2	94.7	>128	>128	>128	>128
4	50.5	>12.8 ≤ 128	>12.8 ≤ 128	>1.28 ≤ 12.8	>12.8 ≤ 128
ethambutol[a]		2−4	4−8	4−8	4−8

[a] Historical MIC values.

Table 4. Activity of **2** and **4** against a Panel of Human Tumor Cell Lines

	IC_{50} (μg/mL)[a]						
cmpd	SNB-7	DLD-1	NCI-H23	ZR-75-1	LOX IMVI	PC-3	CAKI-1
2	>60	>60	45	30	29	31	50
4	5.7	11	4.8	5.6	7.8	5.9	6.3
methotrexate	>60	>60	0.29	>60	0.057	0.027	>60

[a] 72-Hour exposure to compound.

Table 5. Tissue Boron Concentrations for Carborane **2**

	μg B/g wet tissue					
time (hr)	animal	blood	brain	tumor	liver	lung[a]
3	1	8.6	8.6	10.8	108.6	25.9
	2	8.1	11.4	0	109.2	31.9
	3	14.1	3.8	2.7	98.9	37.3
16	1	0	9.7	1.6	0	16.2
18	1	0	14.1		19.5	3.8
	2	0	6.5		7.1	27.0

[a] These values are probably high due to the low tissue weights and the fact that the compound is unenriched.

3- to 10-fold greater activity depending on the cell line tested (Table 4). Compound **2** was significantly less active than **4** against hDHFR, its putative target, and showed significantly less toxicity in the panel of human tumor cell lines. This fact, and the lower logP value (indicating potentially better solubility), suggested that **2** would be a better agent for delivery of boron as a candidate for BNCT. Ideally high levels of boron would be delivered to the tumor site with minimal toxic side effects to, and low boron levels in, normal tissue. Although this compound does exhibit toxicity, the rationale at the time was that the antifolate effects might possibly be mediated by concomitant administration of leucovorin in a regimen that would allow maximum delivery of boron to tumor tissue while rescuing normal tissue from the antifolate effects. Unfortunately, the data with *L. casei* suggest that these compounds might have other, toxic effects outside of DHFR inhibition. This possibility, however, remains to be proven with human cells. Regardless, the data for boron tissue distribution (Table 5) at any specific time point suggest that sample **2** shows relatively poor ratios of boron in tumor tissue/boron in normal tissue, and this is also true for the boron in tumor tissue/boron in brain tissue ratio. Inoperable brain tumors are considered to be one of the primary candidates for this type of treatment. Hence, **2** cannot be considered as a good candidate for BNCT.

Human DHFR/NADPH/Carborane Ternary Complex Crystal Structures. We determined the crystal structures of both carboranes **2** and **4** bound to hDHFR to gain insight into how these unusual TMP analogues were accommodated by the enzyme, and to understand better their improved activity compared to TMP. The hDHFR/NADPH ternary complexes with both carboranes crystallized with two complexes per asymmetric unit. X-ray diffraction data for the *nido*-carborane **2** ternary complex extended to 1.5 Å resolution, and data from the *closo*-carborane **4** ternary complex extended to 1.4 Å. Both structures were solved using molecular replacement, and the NADPH and inhibitors in both structures were built into unambiguous electron density. Refinement, including individual anisotropic temperature factors, resulted in final free-R factors of 21.3% (carborane **2**) and 20.2% (carborane **4**; see Supporting Information, Table S1). Because the overall structures of the ternary complexes agree in large part with previously published models of hDHFR,[20] only the aspects of inhibitor binding will be discussed here.

Carborane Cages are Bound in a Single Rotational Orientation. The most unanticipated and interesting feature of these two structures is that the carborane cages of both **2** and **4** are bound in the DHFR active site in a single rotational orientation. Because icosahedral carboranes can be thought of as rotationally averaged phenyl groups, we had expected to observe rotationally disordered carborane cages attached to well-ordered diaminopyrimidine groups. Surprisingly, however, each carborane is observed to adopt a unique orientation, both in overall rotation around the carborane C1C−B12 pseudosymmetry axis (see Scheme 1 for atom numbering of the carborane cage) as well as with respect to 5-fold rotation about this axis from one orientation to another pseudosymmetrical one. As shown in Figure 1, the unique cage carbon C2C in the *closo*-carborane **4** complex adopts a single position, centered 4.7 Å above the C3 and C4 atoms of the NADPH dihydropyridine ring. Alternative pseudosymmetrical orientations are ruled out by examination of the difference Fourier maps (Supporting Information, Figure S1), which allow clear discrimination between the C2C carbon atom and the less electron-dense boron atoms.

Similarly, the "open" cage position in *nido*-carborane **2**, that is, where the missing boron atom B3 would be located (Scheme 1), also adopts a single orientation, this time pointing roughly away from the NADPH dihydropyridine ring. The cage in carborane **2** is chiral due to asymmetric substitution around the cage C1C carbon; it was synthesized as the racemic mixture. Early in the crystallographic refinement, difference Fourier maps as well as uneven temperature factors for cage atoms clearly indicated that both enantiomers of **2** were bound to DHFR, apparently in equal amounts. Thus, in the final stages of refinement, a 1:1 mixture of the enantiomers was modeled, which equalized the relevant temperature factors. In both enantiomers, the cage carbon C2C adopts a position distinct from that found in carborane **4**.

Both carborane cages make van der Waals interactions with the NADPH nicotinamide group as well as with several DHFR side chains, with increasing distances to Phe-34 (~3.3 Å), Phe-31, Ile-60, Thr-56, and Leu-22 (~4.7 Å).

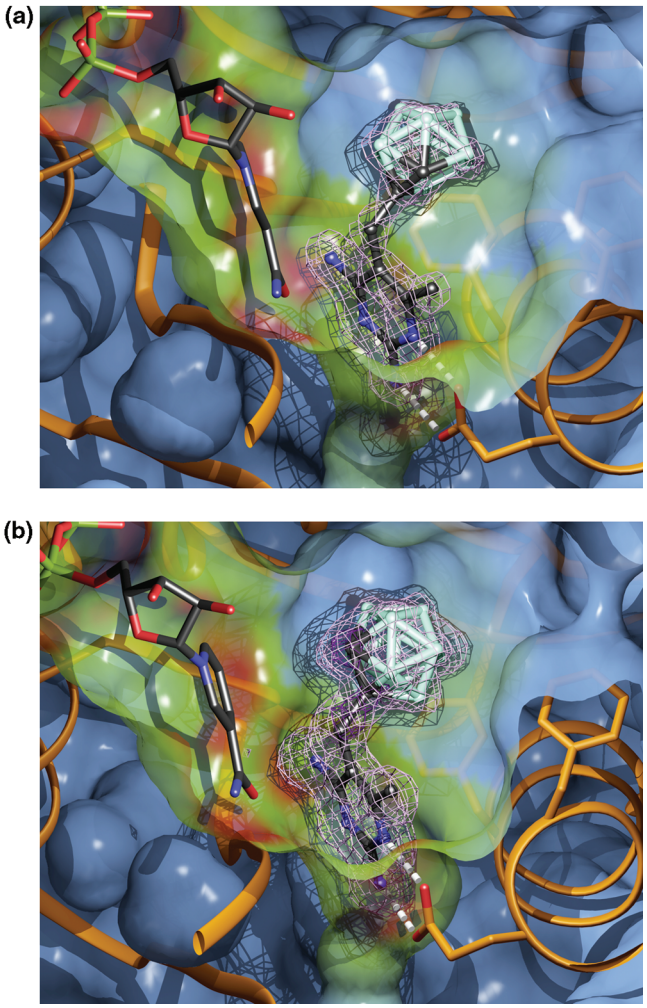

Figure 1. The carborane cages of compounds **2** and **4** adopt a single conformation when bound to hDHFR. (a, b) Carboranes **2** (a) and **4** (b) are shown as found in the hDHFR/NADPH ternary complexes; only a single enantiomer of the bound racemate is shown for **2**. The 1.5 Å resolution F_O-F_C electron density maps, showing positive electron density in the active site prior to inclusion of either inhibitor in the molecular models, are shown at 3.5σ above the mean density for **2** (light purple mesh) and 2.0σ and 4.5σ (dark purple) for **4**. Ligands are multicolored (B, light green; C, black; N, blue; O, red; P, yellow-green). The hDHFR Cα trace is shown as an orange ribbon, and the side chains of residues Glu-30, Phe-31, and Phe-34 are shown; hydrogen bonds between the diaminopyrimidine group and Glu-30 are represented by dashed white bars. The protein solvent accessible surface is colored according to distance to the ligands (0 Å, red; 0.5 Å, yellow; >3.5 Å, blue).

Steric considerations alone indicate that the *closo*-carborane **4** should be rotationally disordered—each of the 10 equatorial cage atoms has an attached hydrogen atom. Therefore, the observed unique cage conformation must arise from electronic factors. Although the cage in *nido*-carborane **2** is not symmetrical, it was somewhat surprising that it bound in a single (enantiomeric) conformation as well.

To understand better these electronic factors, ab initio calculations were carried out at the 6-31+G* level of theory[21−23] to provide the atomic charge distributions and dipole moments for the inhibitors (see Supporting Information, Figure S2). Calculations used the hDHFR-bound conformations of the inhibitors, protonated at N1; hydrogen atoms were included as found in the small-molecule crystal structures of **2** and precursor carborane **1**. The inhibitors exhibit strong dipole moments, with the (expected negatively charged) partial carborane cage in **2** negative (−0.92) and the protonated 2,4-diamino-6-methylpyrimidine group positive (+0.64); the full cage of **4** is more neutral (−0.08), and the protonated 2,4-diamino-6-methylpyrimidine group is again quite positive (+0.90). As expected from atomic electronegativity values, the cage hydrogen atoms attached to boron tend to have slightly negative partial charges (mean values of −0.08 and −0.03 for **2** and **4**), whereas the boron atoms are positive (**2**, +0.07; **4**, +0.45); the hydrogen attached to cage carbon C2C has a pronounced positive partial charge (**2**, +0.11; **4**, +0.20).

We conclude that the rotational preferences for both carborane cage types arise from the detailed electrostatic interactions between the nonuniformly charged carborane cages and the characteristic partial atomic charges and, hence, electric field, found in the solvated hDHFR active site. Additional work to further probe this point, for example, Poisson−Boltzmann calculations with rotationally distinct inhibitor cage orientations in the context of the fully solvated protein, were deemed unlikely to shed much more light on the matter and were not pursued.

Carborane Antifolates and Trimethoprim Exhibit Similar Binding Modes. The location of compounds **2** and **4** bound in the hDHFR active site, as well as their molecular conformations, are essentially identical to that of TMP (Figure 2).[24,25] The diaminopyrimidine groups of both carboranes are bound in well-defined orientations that overlay the position adopted by TMP. In the *closo*-carborane **4** complex, N1 and N2 make tight hydrogen bonds (2.65 and 2.8 Å) with the side chain carboxylate of Glu-30 (Figure 1). N4 makes a weak hydrogen bond (3.15 Å) with the carbonyl oxygen of Ile-7, and more distant van der Waals interactions with the carbonyl oxygen atoms of nicotinamide and Val-115, and the side chain Oη of Tyr-121. The methylene and methyl groups bonded to C5 and C6 are in van der Waals contact with the nicotinamide C3 and the side chain of Leu-22, respectively. Essentially identical interaction distances are observed in the *nido*-carborane **2** complex. An alternative diaminopyrimidine orientation, with this group rotated by ∼180°, thereby exchanging N4 and the methyl group (and N1/N3), was conclusively ruled out by a test refinement. With the rotated model, the free R-factor increased by ∼1%, and the difference in temperature factors between the exocyclic amino (N4) and methyl (C6′) atoms increased from ∼1.5 Å^2 to 5 Å^2, with N4 being lower than C6′.

Hydrogen bonding and van der Waals interactions equivalent to those described above for compounds **2** and **4** were observed in the chicken DHFR/NADPH/TMP ternary complex;[25] the hDHFR ternary complex is also equivalent (A.K.W.L. and D.W.B., unpublished results). In the *E. coli* DHFR/TMP binary complex, however, an additional strong hydrogen bond (∼2.8 Å) between N4 and the carbonyl oxygen atom of Ile-94 (Val-115 in hDHFR) was observed.[25]

The TMP conformation is defined by the two dihedral angles around the TMP "benzyl" carbon (C7): θ_1 (C4−C5−C7−C1′) and θ_2 (C5−C7−C1′−C2′) (Figure 2). In the chicken DHFR/NADPH/TMP ternary complex, these angles are $\theta_1 = -85°$ and $\theta_2 = 102°$;[25] angles of $\theta_1 = -95°$ and $\theta_2 = 95°$ are observed in the hDHFR ternary complex (A.K.W.L. and D.W.B., unpublished results). For the carborane inhibitors, with θ_1 and θ_2 defined analogously (θ_1, C4−C5−C5′−C1C; θ_2, C5−C5′−C1C−B5; B5 of the carborane cage is closest to C2′ of TMP), the values are $\theta_1 = -97°$ and $\theta_2 = 100°$ (compound **2**) and $\theta_1 = -88°$ and $\theta_2 = 103°$ (compound **4**). As observed previously, all these dihedral values are distinct from those observed in DHFR/TMP binary complexes, for example, $\theta_1 = 177°$ and $\theta_2 = 76°$ in the *E. coli* DHFR/TMP complex.[25]

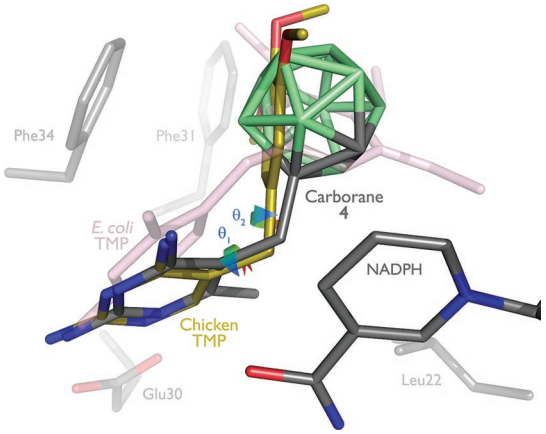

Figure 2. TMP and the carboranes **2** and **4** bind similarly to hDHFR. Carborane **4** (coloring as in Figure 1) is shown with selected hDHFR active site side chains and NADPH. TMP bound to chicken DHFR/NADPH,[25] with the human and chicken enzymes aligned, is shown also (yellow C atoms). The torsion angles θ_1 and θ_2 (defined in the text)[24] are illustrated as multicolored arrows surrounding the relevant TMP bonds. Note the essentially similar orientation and torsion angles between the two inhibitors. By contrast, TMP bound to *E. coli* DHFR (pink C atoms)[25] adopts very different θ_1 and θ_2 values.

One difference between the carboranes and TMP when bound to DHFR is the magnitude of solvent accessible surface area (ASA) that is buried. For TMP, 450 Å^2 of ASA is buried upon binding, that is, ∼90% of the total inhibitor surface area. About 230 Å^2 of DHFR/NADPH ASA is made inaccessible by TMP, for a total buried ASA of 680 Å^2. For both compounds **2** and **4**, by contrast, about 390 Å^2 (out of 420 Å^2 total) of inhibitor ASA is buried upon binding. For the protein, slightly less (210 Å^2) surface area becomes inaccessible, for a total buried ASA of 600 Å^2. Somewhat unexpected from these differences in buried ASA between TMP and the carboranes, namely, ∼80 Å^2, that is, 12% of the ASA buried upon TMP binding, the carboranes are actually the more potent inhibitors (Table 2). The improved potency of carboranes **2** and **4** is not due to the presence of the 6-CH_3 group, as 6-CH_3-TMP is actually ∼2-fold worse an inhibitor than is TMP itself (Table 2).[26]

Concluding Remarks

Carboranes **2** and **4** were only moderately active in the screens presented herein and are not candidates for antimicrobial or anticancer chemotherapy. Neither are they viable BNCT candidates. The carborane substitution sterically approximates a phenyl ring rotated in three-dimensional space, and it was interesting to determine how this substitution would be tolerated within the DHFR active site. The crystal structures of **2** and **4** bound to hDHFR showed that both compounds bind in a manner very similar to the prototypical 2,4-diamino-5-benzylpyrimidine, TMP, placing the carborane cages in the same region as the TMP phenyl ring. Because this region is critical to binding and antibacterial selectivity, it was interesting to ascertain the effects of this substitution on antibacterial activity and selectivity. A similar approach has been taken relative to anticancer antifolates. In the active 2,4-diamino-6-methyl-5-(3,4-dichlorophenyl)-substituted pyrimidine antifolate, metoprine, the 5-(3,4-dichlorophenyl) group was replaced with an adamantyl group leading to more potent inhibitors.[27] It is clear from our data that the carborane-substituted analogs **2** and **4** are sterically tolerated in relation to inhibiting the DHFR enzymes studied. In fact, these analogs are nonselective, micromolar inhibitors similar in activity to 2,4-diamino-5-benzylpyrimidine,[28,29] and the added hydrophobic surface area and potential active site occupancy does not appear to improve enzyme inhibition.

The data against *T. gondii* DHFR are interesting, however, in that *nido*-carborane **2** shows significant (nanomolar) activity against this enzyme. The activity of **2** is about 2-fold greater than **4** against this DHFR, and **2** is approximately 65-fold more selective for *T. gondii* DHFR versus the rat liver protein. In every other case, compound **4** is more active against the DHFR tested than **2** by ratios ranging from 2 (*P. carinii*) up to 58 (*L. casei*). Although there may be a unique capability of the *T. gondii* enzyme to accommodate the open, *nido*-carborane better than the closed, *closo*-carborane, structurally, **2** and **4** are very similar; the primary difference lies in the negative charge on the *nido*-carborane cage. Possibly, there is a unique feature within the *T. gondii* DHFR that can accommodate this charge with little impact on enzyme inhibition, whereas in the case of the rat liver or human enzymes, binding of **2** is reduced by a factor of 10 or more. This difference might be exploitable for the design of more selective antifolates against *T. gondii*.

Experimental Section

Biological Evaluation. Inhibition of Dihydrofolate Reductase. DHFR from both *Lactobacillus casei* (30% pure) and the human recombinant enzyme were assayed according to procedures reported by Kisliuk et al.[30] The pure human recombinant enzyme was supplied by Prof. J. H. Freisheim.[31] IC_{50} values for DHFR from *P. carinii*, *T. gondii*, *M. avium*, and rat liver were determined as reported.[32,33] Independently, the activities versus *M. avium* were determined using purified recombinant *M. avium* DHFR[34] by reported methods.[35,36]

In Vitro Inhibition of Bacterial Growth. The inhibition of growth was determined for *L. casei* (ATCC 7469), *M. tuberculosis* H37Ra (ATCC 25177), and three *M. avium* strains by compounds **2** and **4** (Table 2). The *M. avium* strains were clinical isolates obtained from the National Jewish Center for Immunology and Respiratory Diseases, Denver, CO. *L. casei* inhibition was determined turbidimetrically with a macrodilution broth assay according to Bakerman.[37] The inhibition of growth of the mycobacterial strains was determined using a colorimetric microdilution broth assay and 10-fold serial dilutions of drug, as described elsewhere.[38] The MIC is defined as the lowest amount of drug that inhibited growth completely.

Evaluation as Anticancer Agents: Activity in a Panel of Human Tumor Cell Lines. The cell lines CAKI-1 (renal), DLD-1 (colon), NCI-H23 (lung), ZR-75−1 (mammary), SNB-7 (CNS), PC-3 (prostate), and LOX IMVI (melanoma) were propagated using standard tissue culture techniques in RPMI 1640 media with 10% FBS, and 2 mM L-glutamine at 37 °C with 5% CO_2 and humidity control. IC_{50} values were determined as reported.[38]

Evaluation as Candidates for Boron Neutron Capture Therapy. Preliminary BNCT experiments were performed using compound **2** as it was the least overtly toxic (see Table 3) of the two carboranes. All injections were intraperitoneal into BALB/c mice. Harding−Passey melanomas were carried subcutaneously on the abdomen. Two solutions were used for the experiment. The first solution was 22.5 mg of **2** in 4.0 mL of 50% aqueous propylene glycol. The second solution contained a higher amount of **2** at 45.0 mg in 4.0 mL of 50% aqueous propylene glycol. The first solution was analyzed by the prompt γ method,[39] and contained 1642.7 μg B/mL. The second solution was not analyzed by prompt γ, but the amount of boron received by the animals was approximated based on results from the other solution. Using the first solution, three tumor-bearing mice received approximately 17 μg B per gram of body weight (gbw), all appeared healthy and were sacrificed at 3 h. The second solution was used in the following treatments. Two nontumor mice received 33 μg B/gbw, the highest dose administered. Both were dead within 1 h. Three tumor-bearing mice received approximately 24 μg B/gbw; two were dead by the following morning, and the third appeared healthy and was sacrificed at 16

h. Finally, two nontumor animals received approximately 16 μg B/gbw. Both lived, looked healthy, and were sacrificed at 18 h. Tissues were harvested and analyzed by prompt γ to determine tissue boron concentration. Data for the surviving, healthy animals that were sacrificed at the 3, 16, and 18 h time points are presented in Table 5. It is notable that the maximum tolerated dose appears to be in the 16−17 μg B/gbw. Hence, although the lone, surviving animal (receiving 24 μg B/gbw) in the 16 h experiment appeared quite normal, the data at this time point may be questionable due to the fact that two out of three of the animals died at this higher dose.

Acknowledgment. These studies were supported in part by the National Institutes of Health Grants AI-41348, AI-38667, and AI-45317. We would also like to acknowledge the excellent technical assistance of Louise Westbrook and Kenneth Wright. We thank Prof. Steve Ealick (Cornell Univ.) for determining the crystal structures of compounds **1** and **2**; these coordinates were used in modeling the inhibitors in the hDHFR active site and in the quantum calculations. We also thank David Matthews (Pfizer, La Jolla, CA) for providing the chicken DHFR/NADPH/TMP ternary complex and *E. coli* DHFR/TMP binary complex coordinates. D.W.B. was supported by NIH Grants AI-30279 and AI-38707 (P.I.: James R. Piper).

Supporting Information Available: Additional synthetic chemistry, crystallographic, and modeling experimental details; illustrations of experimental electron density and calculated partial atomic charges for carboranes **2** and **4**. This material is available free of charge via the Internet at http://pubs.acs.org.

References

(1) Costi, M. P.; Ferrari, S. Update on antifolate drugs targets. *Curr. Drug Targets* **2001**, *2*, 135−166.
(2) Takimoto, C. H.; Allegra, C. J. New antifolates in clinical development. *Oncology* **1995**, *9*, 649−656, 659 DISC 660, 662, 665.
(3) Takemura, Y.; Kobayashi, H.; Miyachi, H. Antifolate resistance and its circumvention by new analogues. *Hum. Cell* **2001**, *14*, 185−202.
(4) Calvert, H.; Bunn, P. A., Jr. Future directions in the development of pemetrexed. *Semin. Oncol.* **2002**, *29*, 54−61.
(5) Periti, P. Brodimoprim, a new bacterial dihydrofolate reductase inhibitor: A minireview. *J. Chemother.* **1995**, *7*, 221−223.
(6) Warhurst, D. C. Resistance to antifolates in *Plasmodium falciparum*, the causative agent of tropical malaria. *Sci. Prog.* **2002**, *85*, 89−111.
(7) Sato, E. I. Methotrexate therapy in systemic lupus erythematosus. *Lupus* **2001**, *10*, 162−164.
(8) Walker, V. K.; Tyshenko, M. G.; Kuiper, M. J.; Dargar, R. V.; Yuhas, D. A.; Cruickshank, P. A.; Chaguturu, R. Tobacco budworm dihydrofolate reductase is a promising target for insecticide discovery. *Eur. J. Biochem.* **2000**, *267*, 394−403.
(9) Reynolds, R. C.; Johnson, C. A.; Piper, J. R.; Sirotnak, F. M. Synthesis and antifolate evaluation of the aminopterin analogue with a bicyclo[2.2.2]octane ring in place of the benzene ring. *Eur. J. Med. Chem.* **2001**, *36*, 237−242.
(10) Grimes, R. N. *Carboranes*; Academic Press: New York, 1970.
(11) Hitchings, G. H.; Baccanari, D. P. Design and synthesis of folate antagonists as antimicrobial agents. In *Folate Antagonists as Therapeutic Agents. Volume I, Biochemistry, Molecular Actions and Synthetic Design*; Sirotnak, F. M., Burchall, J. J., Ensminger, W. B., Montgomery, J. A., Eds.; Academic Press: New York, 1984; pp 151−172.
(12) Barth, R. F.; Soloway, A. H.; Goodman, J. H.; Gahbauer, R. A.; Gupta, N.; Blue, T. E.; Yang, W.; Tjarks, W. Boron neutron capture therapy of brain tumors: An emerging therapeutic modality. *Neurosurgery* **1999**, *44*, 433−451; discussion 450−451, review.
(13) Hawthorne, M. F. New horizons for therapy based on the boron neutron capture reaction. *Mol. Med. Today* **1998**, *4*, 174−181.
(14) Gahbauer, R.; Gupta, N.; Blue, T.; Goodman, J.; Barth, R.; Grecula, J.; Soloway, A. H.; Sauerwein, W.; Wambersie, A. Boron neutron capture therapy: Principles and potential. *Recent Res. Cancer Res.* **1998**, *150*, 183−209.
(15) Barth, R. F.; Yang, W.; Adams, D. M.; Rotaru, J. H.; Shukla, S.; Sekido, M.; Tjarks, W.; Fenstermaker, R. A.; Ciesielski, M.; Nawrocky, M. M.; Coderre, J. A. Molecular targeting of the epidermal growth factor receptor for neutron capture therapy of gliomas. *Cancer Res.* **2002**, *62*, 3159−3166.
(16) Reynolds, R. C.; Trask, T. W.; Sedwick, W. D. 2,4-Dichloro-5-(1-o-carboranylmethyl)-6-methylpyrimidine: A potential synthon for 5-(1-*o*-carboranylmethyl)pyrimidines. *J. Org. Chem.* **1991**, *56*, 2391−2395.
(17) Wiesboeck, R. A.; Hawthorne, M. F. Dicarbaundecaborane(13) and derivatives. *J. Am. Chem. Soc.* **1964**, *86*, 1642−1643.
(18) Maiti, S. N.; Singh, M. P.; Micetich, R. G. Facile conversion of azides to amines. *Tetrahedron Lett.* **1986**, *27*, 1423−1424.
(19) Imamura, K.-i.; Yamamoto, Y. Synthesis and in vitro evaluation of 5-closo- and 5-nido-orthocarboranyluridines as boron carriers. *Bull. Chem. Soc. Jpn.* **1997**, *70*, 3103−3110.
(20) Klon, A. E.; Heroux, A.; Ross, L. J.; Pathak, V.; Johnson, C. A.; Piper, J. R.; Borhani, D. W. Atomic structures of human dihydrofolate reductase complexed with NADPH and two lipophilic antifolates at 1.09 Å and 1.05 Å resolution. *J. Mol. Biol.* **2002**, *320*, 677−693.
(21) Chandrasekhar, J.; Andrade, J. G.; Schleyer, P. v. R. Efficient and accurate calculation of anion proton affinities. *J. Am. Chem. Soc.* **1981**, *103*, 5609−5612.
(22) Spitznagel, G. W.; Clark, T.; Chandrasekhar, J.; Schleyer, P. v. R. Stabilization of methyl anions by first-row substituents. The superiority of diffuse function-augmented basis sets for anion calculations. *J. Comput. Chem.* **1982**, *3*, 363−371.
(23) Clark, T.; Chandrasekhar, J.; Spitznagel, G. W.; Schleyer, P. v. R. Efficient diffuse function-augmented basis sets for anion calculations. III. The 3−21 + G basis set for first-row elements, lithium to fluorine. *J. Comput. Chem.* **1983**, *4*, 294−301.
(24) Matthews, D. A.; Bolin, J. T.; Burridge, J. M.; Filman, D. J.; Volz, K. W.; Kraut, J. Dihydrofolate reductase. The stereochemistry of inhibitor selectivity. *J. Biol. Chem.* **1985**, *260*, 392−399.
(25) Matthews, D. A.; Bolin, J. T.; Burridge, J. M.; Filman, D. J.; Volz, K. W.; Kaufman, B. T.; Beddell, C. R.; Champness, J. N.; Stammers, D. K.; Kraut, J. Refined crystal structures of Escherichia coli and chicken liver dihydrofolate reductase containing bound trimethoprim. *J. Biol. Chem.* **1985**, *260*, 381−391.
(26) Roth, B.; Aig, E.; Lane, K.; Rauckman, B. S. 2,4-Diamino-5-benzylpyrimidines as antibacterial agents. 4. 6-Substituted trimethoprim derivatives from phenolic Mannich intermediates. Application to the synthesis of trimethoprim and 3,5-dialkylbenzyl analogues. *J. Med. Chem.* **1980**, *23*, 535−541.
(27) Werbel, L. M. Design and synthesis of lipophilic antifols as anticancer agents. In *Folate Antagonists as Therapeutic Agents. Volume I, Biochemistry, Molecular Actions and Synthetic Design*; Sirotnak, F. M., Burchall, J. J., Ensminger, W. B., Montgomery, J. A., Eds.; Academic Press: New York, 1984; pp 261−287.
(28) Baccanari, D. P.; Kuyper, L. F. Basis of selectivity of antibacterial diaminopyrimidines. *J. Chemother.* **1993**, *5*, 393−399.
(29) Hartman, P. G. Molecular aspects and mechanism of action of dihydrofolate reductase inhibitors. *J. Chemother.* **1993**, *5*, 369−376.
(30) Kisliuk, R. L.; Strumpf, D.; Gaumont, Y.; Leary, R. P.; Plante, L. Diastereoisomers of 5,10-methylene-5,6,7,8-tetrahydropteroyl-D-glutamic acid. *J. Med. Chem.* **1977**, *20*, 1531−1533.
(31) Prendergast, N. J.; Delcamp, T. J.; Smith, P. L.; Freisheim, J. H. Expression and site-directed mutagenesis of human dihydrofolate reductase. *Biochemistry* **1988**, *27*, 3664−3671.
(32) Broughton, M. C.; Queener, S. F. Pneumocystis carinii dihydrofolate reductase used to screen potential antipneumocystis drugs. *Antimicrob. Agents Chemother.* **1991**, *35*, 1348−1355.
(33) Chio, L. C.; Queener, S. F. Identification of highly potent and selective inhibitors of *Toxoplasma gondii* dihydrofolate reductase. *Antimicrob. Agents Chemother.* **1993**, *37*, 1914−1923.
(34) Zywno-van-Ginkel, S.; Dooley, T. P.; Suling, W. J.; Barrow, W. W. Identification and cloning of the *Mycobacterium avium* folA gene, required for dihydrofolate reductase activity. *FEMS Microbiol. Lett.* **1997**, *156*, 69−78.
(35) Suling, W. J.; Reynolds, R. C.; Barrow, E. W.; Wilson, L. N.; Piper, J. R.; Barrow, W. W. Susceptibilities of Mycobacterium tuberculosis and Mycobacterium avium complex to lipophilic deazapteridine derivatives, inhibitors of dihydrofolate reductase. *J. Antimicrob. Chemother.* **1998**, *42*, 811−815.
(36) Suling, W. J.; Seitz, L. E.; Pathak, V.; Westbrook, L.; Barrow, E. W.; Zywno-van-Ginkel, S.; Reynolds, R. C.; Piper, J. R.; Barrow, W. W. Antimycobacterial activities of 2,4-diamino-5-deazapteridine derivatives and effects on mycobacterial dihydrofolate reductase. *Antimicrob. Agents Chemother.* **2000**, *44*, 2784−2793.
(37) Bakerman, H. A. A method for measuring the microbiological activity of tetrahydrofolic acid and other labile reduced folic acid derivatives. *Anal. Biochem.* **1961**, *2*, 558−567.

(38) Reynolds, R. C.; Tiwari, A.; Harwell, J. E.; Gordon, D. G.; Garrett, B. D.; Gilbert, K. S.; Schmid, S. M.; Waud, W. R.; Struck, R. F. Synthesis and evaluation of several new (2-chloroethyl)nitrosocarbamates as potential anticancer agents. *J. Med. Chem.* **2000**, *43*, 1484−1488.

(39) Fairchild, R. G.; Gabel, D.; Laster, B. H.; Greenberg, D.; Kiszenick, W.; Micca, P. L. Microanalytical techniques for boron analysis using the ^{10}B(n,alpha)^{7}Li reaction. *Med. Phys.* **1986**, *13*, 50−56.

JM0701977